Multi-configurational short-range density functional theory can describe spin–spin coupling constants of transition metal complexes

Kjellgren, Erik Rosendahl; Jensen, Hans Jørgen Aagaard

Published in:
The Journal of Chemical Physics

DOI:
10.1063/5.0059128

Publication date:
2021

Document version:
Accepted manuscript

Multi-configurational short-range density-functional theory can describe spin-spin coupling constants of transition metal complexes

Erik Rosendahl Kjellgren[1, a)] and Hans Jørgen Aagaard Jensen[1]
Department of Physics, Chemistry and Pharmacy, University of Southern Denmark, DK-5230 Odense M, Denmark

(*Electronic mail: hjj@sdu.dk)

(Dated: 3 August 2021)

The multi-configurational short-range density functional theory (MC–srDFT) has been extended to the calculation of indirect spin-spin coupling constants (SSCCs) for NMR spectroscopy. The performance of the new method is compared to Kohn-Sham density functional theory (KS–DFT) and *ab initio* CASSCF for a selected set of molecules with good reference values. Two families of density functionals are considered, the local density approximation (sr)LDA and the generalized gradient approximation (sr)PBE. All srDFT calculations are of Hartree-Fock type or complete active space type, HF–srDFT or CAS–srDFT. In all cases the calculated SSCC values are of the same quality for srLDA and srPBE functionals, suggesting one should use the computationally cheaper srLDA functionals in applications. For all calculated SSCCs in organic compounds the best choice is HF–srDFT, the more expensive CAS–srDFT does not provide better values for these single-reference molecules. Fluorine is a challenge, in particular FF, FC and FO couplings have much higher statistical errors than the rest. For SSCCs involving fluorine and a metal atom CAS–srDFT with singlet gTDA is needed to get good SSCC values although the reference ground state is not a multi-reference case. For VF_6^{-1} all other considered models fail blatantly.

I. INTRODUCTION

Nuclear magnetic resonance (NMR) is one of the most powerful tools available to characterize the molecular structures in an experimental setting, due to the NMR parameters sensitivity to the electronic structure. This makes NMR a crucial tool for identifying known compounds and determining the structure of new compounds. An import component of the NMR parameters is the indirect nuclear spin-spin coupling constants (SSCCs). For new compounds, the interpretation of experimental NMR results can be difficult, especially for inorganic complexes. Accurate calculations of SSCCs thus have great importance for theoretical aided interpretation of experimental NMR.[1–3]

The non-relativistic theoretical model for SSCC is a combination of four contributions, as first derived by Ramsey,[4] the diamagnetic spin-orbit coupling (DSO), the paramagnetic spin-orbit coupling (PSO), the Fermi contact coupling (FC), and the spin-dipole coupling (SD) contribution. Here the DSO terms are expectation values, PSO requires imaginary singlet response equations to be solved, and the FC and SD require real triplet response equations to be solved.[1] For many types of SSCCs, the FC coupling is by far the most dominant term but the other terms cannot be ignored for a robust prediction of SSCCs, as-is once again documented in the results section below.

Calculations of SSCCs have been developed for many different electron-structure theory approaches[5–8]. The most widely used methods, also for SSCCs, are various Kohn-Sham density functional theory (KS-DFT) methods due to their computationally efficient treatment of the Coulomb hole, the short-range dynamical electron-electron correlation,[9] compared to *ab initio* methods. For KS-DFT models for SSCCs we point to the pioneering works of Malkin *et al.*[10] and Dickson *et al.*[11] Seeking higher accuracy and ways to systematically improve calculated properties, SSCCs have also been implemented for the correlated wave-function methods Second-Order Polarization Propagator Approach (SOPPA),[12–15] Algebraic Diagrammatic Construction (ADC),[16] coupled cluster models (in particular CC2, CC3, CCSD),[17–21] and multi-configurational self-consistent field (MCSCF)[22,23]. Notable here is that of these methods, only MCSCF can tackle multi-reference molecules, that is, molecules with significant static correlation effects.

In summary, the situation today is that for single-reference molecules one usually can obtain accurate results with CC3 and CCSD, and fairly accurate results with SOPPA, CC2, and some KS-DFT functionals. For multi-reference molecules, only MCSCF models have been applicable hitherto, however, with limited accuracy because the dynamic electron-electron short-range correlation cannot be satisfactorily described with MCSCF, not only because the number of configurations becomes too big, but also because the variational optimization of an MCSCF wave function is numerically difficult for the weakly occupied orbitals needed for dynamic correlation (the energy change is very small when these orbitals are attempted to be optimized).

In this work we propose a new computational model for SSCCs (J_{KL}) by replacing MCSCF with multi-configurational short-range density functional theory (MC-srDFT), which can describe both static (multi-reference) and dynamic correlation effects. In short, the long-range MCSCF part can describe static correlation, while the short-range DFT part can describe the dynamic correlation. We have previously published implementations of MC–srDFT linear response for excitation energies, both for singlet[24] and triplet[25] excitations. We have ex-

a)Department of Physics, Chemistry and Pharmacy, University of Southern Denmark, DK-5230 Odense M, Denmark.

tended this code to MC–srDFT calculations of linear response equations, which we here employ for the FC, SD, and PSO terms. We exploited the existing framework in Dalton[26] for calculation of SSCCs with MCSCF[22] to keep track of all the individual contributions for the MC–srDFT model.

In this paper, we first describe our implementation for MC–srDFT to calculations of indirect spin-spin coupling constants, which has been released in Dalton2020.[27] We evaluate its performance for a benchmark set of small molecules and a series of transition metal complexes. In this context, we also investigate whether one should invoke the generalized Tamm-Dancoff approximation gTDA[25], which we previously found improved the lowest triplet excitation energies because of near triplet instabilities.[25]

In the following sections, we summarize the theory, describe computational details, present and discuss computational results, and finish with conclusions.

II. THEORETICAL SUMMARY

We here shortly recapitulate the theory and formulae for indirect spin-spin coupling calculations for singlet reference molecules and MC–srDFT singlet and linear response theory.

A. Indirect spin-spin coupling in NMR

The usual spin-Hamiltonian in terms of nuclear spin operators $\hat{\mathbf{I}}_K$ for interpretation of NMR of non-paramagnetic molecules with singlet electronic spin is[28]

$$\hat{\mathbf{H}} = \sum_K \hat{\mathbf{I}}_K \cdot (\mathbf{1} - \boldsymbol{\sigma}_K) \cdot \mathbf{B} + \sum_{K<L} \hat{\mathbf{I}}_K \cdot \mathbf{J}_{KL} \cdot \hat{\mathbf{I}}_L \,, \tag{1}$$

where $\boldsymbol{\sigma}_K$ is the screening tensor and $\mathbf{J}_{KL}$ is the indirect spin-spin coupling tensor. The non-relativistic expression for $\mathbf{J}_{KL}$ consists of four terms (three if you take FC and SD together):[1,2,4]

$$\mathbf{J}_{KL} = \mathbf{J}_{KL}^{\mathrm{DSO}} + \mathbf{J}_{KL}^{\mathrm{PSO}} + (\mathbf{J}_{KL}^{\mathrm{FC}} + \mathbf{J}_{KL}^{\mathrm{SD}}) \tag{2}$$

where the diamagnetic spin-orbit (DSO) term constitutes of six expectation values; the paramagnetic spin-orbit (PSO) contribution requires the solution of three singlet linear response equations; the Fermi contact (FC) contribution requires the solution of one triplet linear response equations; and finally, the spin-dipole (SD) contribution requires the solution of six triplet linear response equations.

The reduced isotope independent SSCCs, $\mathbf{K}_{KL}$ is related to the observed as

$$\mathbf{J}_{KL} = \frac{h}{4\pi^2}\,\gamma_K\,\gamma_L\,\mathbf{K}_{KL} \tag{3}$$

where γ_K is the gyromagnetic factor for isotope K which relates its nuclear spin to its magnetic moment $\mathbf{M}_K = \gamma_K \hbar \mathbf{I}_K$. Often one is only interested in the isotropic value

$$J_{KL} = \frac{1}{3}\mathrm{Tr}(\mathbf{J}_{KL}), \tag{4}$$

and it is the isotropic values we will focus on in this paper, as is usual when proposing new methods for SSCC.

The operators used to construct the four different contributions to the SSCC are

$$\begin{aligned}
\hat{\mathbf{h}}_{KL}^{\mathrm{DSO}} &= \alpha^4 \sum_i \frac{\boldsymbol{r}_{iK}^T \boldsymbol{r}_{iL} \boldsymbol{I} - \boldsymbol{r}_{iK} \boldsymbol{r}_{iL}^T}{r_{iK}^3 r_{iL}^3} \\
\hat{\mathbf{h}}_{K}^{\mathrm{PSO}} &= \alpha^2 \sum_i \frac{\boldsymbol{r}_{iK} \times \boldsymbol{p}_i}{r_{iK}^3} \\
\hat{\mathbf{h}}_{K}^{\mathrm{FC}} &= \frac{8\pi\alpha^2}{3} \sum_i \delta(\boldsymbol{r}_{iK})\, \boldsymbol{s}_i \\
\hat{\mathbf{h}}_{K}^{\mathrm{SD}} &= \alpha^2 \sum_i \frac{3\boldsymbol{r}_{iK} \boldsymbol{r}_{iK}^T - r_{iK}^2 \boldsymbol{I}}{r_{iK}^5} \boldsymbol{s}_i
\end{aligned} \tag{5}$$

The above equations are in atomic units. The MCSCF implementation for SSCC in DALTON, which we have used as a basis for our MC–srDFT implementation, is described in Ref. 22.

B. The MC–srDFT model

Our MC–srDFT model har been described in references 24, 25,29–32. In the framework of MC–srDFT the total energy is the sum of a long-range wave function contribution and a short-range density functional theory contribution:

$$\begin{aligned}
E(\boldsymbol{\lambda}) = &\left\langle \Psi(\boldsymbol{\lambda}) \middle| \hat{H}^{\mathrm{lr},\mu} \middle| \Psi(\boldsymbol{\lambda}) \right\rangle \\
&+ E_{\mathrm{H}}^{\mathrm{sr},\mu}[\rho_{\mathrm{C}}(\boldsymbol{r},\boldsymbol{\lambda})] + E_{\mathrm{xc}}^{\mathrm{sr},\mu}[\boldsymbol{\xi}(\boldsymbol{r},\boldsymbol{\lambda})]
\end{aligned} \tag{6}$$

where $\boldsymbol{\lambda}$ is the parameterization of the wave function. For a multi-configurational wave function the parameters are non-redundant configuration coefficients $\boldsymbol{S}^T = \{S_i\}$ and orbital rotation parameters $\boldsymbol{\kappa}^T = \{\kappa_{pq}\}$, thus giving $\boldsymbol{\lambda}^T = \left(\boldsymbol{S}^T, \boldsymbol{\kappa}^T\right)$. The long-range Hamiltonian contains the usual one-electron operators, the nuclear-nuclear repulsion, and a long-range two-electron interaction:

$$\hat{H}^{\mathrm{lr},\mu} = \sum_{pq} h_{pq} \hat{E}_{pq} + \frac{1}{2} \sum_{pqrs} g_{pqrs}^{\mathrm{lr},\mu} \hat{e}_{pqrs}^{\mathrm{lr},\mu} + V_{\mathrm{NN}} \tag{7}$$

where the singlet one- and two-electron operators are $\hat{E}_{pq} = \hat{a}_{p\alpha}^\dagger \hat{a}_{q\alpha} + \hat{a}_{p\beta}^\dagger \hat{a}_{q\beta}$ and $\hat{e}_{pqrs} = \hat{E}_{pq}\hat{E}_{rs} - \delta_{qr}\hat{E}_{ps}$, respectively. The long-range two-electron interaction used here is ($r_{ij} = \left|\boldsymbol{r}_i - \boldsymbol{r}_j\right|$):

$$\begin{aligned}
g_{pqrs}^{\mathrm{lr},\mu} = &\left\langle \phi_p \phi_r \middle| \hat{g}^{\mathrm{lr},\mu}(\boldsymbol{r}_i, \boldsymbol{r}_j) \middle| \phi_q \phi_s \right\rangle \\
= &\left\langle \phi_p \phi_r \middle| \frac{\mathrm{erf}(\mu\, r_{ij})}{r_{ij}} \middle| \phi_q \phi_s \right\rangle
\end{aligned} \tag{8}$$

in which the extent of the long-range part is controlled by the parameter μ. The idea behind MC-srDFT is to let the long-range MCSCF part take care of the long-range static correlation effects and let the short-range DFT part take care of the dynamic Coulomb-hole correlation effects. We have so far found $\mu = 0.4$ bohr^{-1} to give a good balance between the

long-range MCSCF and the short-range DFT parts[24,25,29,30,32], and thus to provide close to optimal accuracy for the investigated properties. The final accuracy of course depends on the chosen short-range density functional and the configurations included in the MCSCF. Note that a much smaller configuration space is needed for MC–srDFT compared to MCSCF, because the dynamic correlation is described by the srDFT part.

The srDFT contribution is here described in the charge-density and spin-density formalism. In this formalism, the relevant quantities for a short-range generalized gradient approximation (srGGA) functional are $\boldsymbol{\xi} = \{\rho_C, \rho_S, \gamma_{CC}, \gamma_{SS}, \gamma_{CS}\}$.

The first two quantities are the charge density and the spin density. These densities can be constructed from their associated density operators as[33,34]

$$\begin{aligned} \hat{\rho}_C(\boldsymbol{r}) &= \sum_{pq} \Omega_{pq}(\boldsymbol{r}) \hat{O}^C_{pq} \\ \hat{\rho}_S(\boldsymbol{r}) &= \sum_{pq} \Omega_{pq}(\boldsymbol{r}) \hat{O}^S_{pq} \end{aligned} \tag{9}$$

where $\Omega_{pq}(\boldsymbol{r}) = \phi^*_p(\boldsymbol{r})\phi_q(\boldsymbol{r})$ is the overlap distribution and

$$\begin{aligned} \hat{O}^C_{pq} &= \hat{E}_{pq} = \hat{a}^\dagger_{p\alpha}\hat{a}_{q\alpha} + \hat{a}^\dagger_{p\beta}\hat{a}_{q\beta} \\ \hat{O}^S_{pq} &= \hat{T}_{pq} = \hat{a}^\dagger_{p\alpha}\hat{a}_{q\alpha} - \hat{a}^\dagger_{p\beta}\hat{a}_{q\beta} \end{aligned} \tag{10}$$

denotes the one-electron singlet and triplet operators, respectively, This leads to the following construction of the density,

$$\rho_X(\boldsymbol{r}, \boldsymbol{\lambda}) = \langle \Psi(\boldsymbol{\lambda}) | \hat{\rho}_X(\boldsymbol{r}) | \Psi(\boldsymbol{r}) \rangle = \sum_{pq} \Omega_{pq}(\boldsymbol{r}) D^X_{pq}(\boldsymbol{r}) \tag{11}$$

where $D^X_{pq}(\boldsymbol{r})$ is the one-electron reduced density matrix for either charge density $X = C$ or spin density $X = S$. The srGGA gradient quantities are

$$\gamma_{XY} = (\nabla \rho_X) \cdot (\nabla \rho_Y) \, . \tag{12}$$

C. MC–srDFT linear response

A general derivation of MC-srDFT linear response can be found in ref. 30. For any variational wave function model, the linear response equations can be expressed in matrix form as follows[35]

$$\left(\boldsymbol{E}^{[2],\mu,X} - \omega \boldsymbol{S}^{[2],\mu,X} \right) = i \boldsymbol{V}^{[1],\mu,X}_x . \tag{13}$$

where $X = C$ for a singlet property and $X = S$ for a triplet property. The right-hand side is a property gradient vector, which for this work is one of the operators in Eq. (5). One can define such a one-electron perturbation operator in terms of the first-order density matrix.

$$V^{[1],\mu,X}_{x,j} = \int_\Omega v_x(\boldsymbol{r}) \rho^{[1]}_{X,j}(\boldsymbol{r}) \mathrm{d}\boldsymbol{r}, \tag{14}$$

with the density property gradient for a singlet reference state being

$$\begin{aligned} \left(\boldsymbol{\rho}^{[1]}_X(\boldsymbol{r}) \right)^T = \big(&\langle \Psi | \left[\hat{O}^{X,\dagger}_{pq}, \hat{\rho}_X \right] | \Psi \rangle, \langle \Psi | \left[\hat{R}_j, \hat{\rho}_X \right] | \Psi \rangle, \\ &\langle \Psi | \left[\hat{O}^X_{pq}, \hat{\rho}_X \right] | \Psi \rangle, \left\langle \Psi \middle| \left[\hat{R}^\dagger_j, \hat{\rho}_X \right] \middle| \Psi \right\rangle \big) \end{aligned} \tag{15}$$

where $\hat{R}_j = |j\rangle\langle 0|$ is the set of state-transfer operators, constructed from all relevant configurations $|j\rangle$ from the CI space.

The Hessian $\boldsymbol{E}^{[2],\mu,X}$ and the metric $\boldsymbol{S}^{[2],\mu,X}$ are structured in the following way, with μ being implicit to not overburden the notation:

$$\begin{aligned} \boldsymbol{E}^{[2],X} &= \begin{pmatrix} \boldsymbol{A}^X & \boldsymbol{B}^X \\ \boldsymbol{B}^{X,*} & \boldsymbol{A}^{X,*} \end{pmatrix} \\ \boldsymbol{S}^{[2],X} &= \begin{pmatrix} \boldsymbol{\Sigma}^X & \boldsymbol{\Delta}^X \\ -\boldsymbol{\Delta}^{X,*} & -\boldsymbol{\Sigma}^{X,*} \end{pmatrix} \end{aligned} \tag{16}$$

The contribution from the multi-configurational wave function to matrices $\boldsymbol{A}^X$, $\boldsymbol{B}^X$, $\boldsymbol{\Sigma}^X$ and $\boldsymbol{\Delta}^X$ for the linear response equations are as defined in Ref. 36, but utilizing the MC–srDFT wave function instead of the MCSCF wave function. The metric blocks $\boldsymbol{\Sigma}^X$ and $\boldsymbol{\Delta}^X$ are also constructed from the MC–srDFT wave function instead of the MCSCF wave function.

Since the energy of the MC–srDFT model is simply the sum of the long-range and the short-range energies, *cf.* Eq. (6), the Hessian is also constructed as a sum of the long-range and short-range contributions

$$\boldsymbol{E}^{[2],X} = \boldsymbol{E}^{[2],X,\mathrm{lr}} + \boldsymbol{E}^{[2],X,\mathrm{sr}} \tag{17}$$

Here the long-range contribution comes from the wave function part, and the short-range contribution is the kernel contribution from the srDFT part. The short-range part is divided into the Hartree (H) and exchange-correlation (xc) contributions,

$$\boldsymbol{E}^{[2],X,\mathrm{sr}} = \boldsymbol{E}^{[2],X,\mathrm{sr}}_{\mathrm{H}} + \boldsymbol{E}^{[2],X,\mathrm{sr}}_{\mathrm{xc}} \tag{18}$$

The specific form of the srDFT kernel contribution to the singlet linear response equation is described in Ref. 30, and the specific form of the kernel contribution to the triplet linear response equation is described in Ref. 25.

The Tamm-Dancoff approximation (TDA) for single-configurational wave functions and the generalized Tamm-Dancoff approximation (gTDA) for multi-configurational wave functions are obtained by setting the $\boldsymbol{B}$ and Δ matrices to zero in Eq. (16). This has been discussed in further detail in Ref. 25. In the results section below the term "Full $E^{[2]}$" refers to results obtained by using the full expression in Eq. (16).

III. COMPUTATIONAL DETAILS

All KS–DFT, HF–srDFT, CAS–srDFT, and CASSCF calculations were performed using a development version of the DALTON2018 program.[26,37] We have tested the short-range functionals srLDA[38] and srPBEgws[39,40] (abbreviated to srPBE in the following), and compared them to the corresponding Kohn-Sham functionals LDA[41–44] and PBE,[45] as well as CASSCF. All srDFT calculations use $\mu = 0.4$ bohr^{-1} as the range-separation parameter, unless otherwise noted. Abelian point group symmetry (D_{2h} and subgroups) has been used in all calculations.

The geometries for the small organic molecules were obtained from Faber *et al.*[21] The aug-ccJ-pVTZ[46–48] basis sets were used for the calculation of spin-spin coupling constants for the small organic molecules. The reference SSCCs from Faber *et al.*[21] were calculated using CC3/aug-ccJ-pVTZ.

The geometries for the inorganic complexes were obtained from Khandogin and Ziegler[49]. All calculations on the inorganic complexes were performed using the aug-cc-pVTZ-J[14,50–53] basis set. The reference SSCCs are experimentally determined values of first row transition metal complexes,[54–60] the SSCCs were compiled by Khandogin and Ziegler[49]. The ScF_6^{-3}, TiF_6^{-2}, VF_6^{-1}, and $Co(CO)_4^{-1}$ were experimentally in aquatic solution[56,61]. The $Fe(CO)_5$ were experimentally in a *neat* solution[62]. The $V(CO)_6^{-1}$ were experimentally in a THF solution[63].

The ccJ-pVTZ and aug-cc-pVTZ-J basis sets were downloaded from Basis Set Exchange[64–66]. The aug-ccJ-pVTZ was constructed by adding the augmented functions of Kendall *et al.*[47]. No vibrational corrections were calculated for the SSCCs.

Assessing the multi-configurational character of the molecules for selection of active orbitals has been done using natural orbital occupations (NOOs) from MP2-srDFT, the MC–srDFT version of using MP2 NOOs for selection of active obitals in MCSCF.[67] Based on MP2–srPBE NOOs with $\mu = 1.0$ bohr^{-1}, the chosen CAS for $V(CO)_6^{-1}$, $Fe(CO)_5$ and $Co(CO)_4^{-1}$ are (10, 16), (10, 10) and (10, 10), respectively. For the selected active orbitals, their MP2–srPBE NOOs for $V(CO)_6^{-1}$ range between 1.86 to 1.96 for the strongly occupied orbitals and between 0.027 to 0.085 for the weakly occupied orbitals. For $Fe(CO)_5$ the two NOO ranges are 1.91 to 1.95 and 0.038 to 0.082, and for $Co(CO)_4^{-1}$ they are 1.90 to 1.93 and 0.070 to 0.093. Clearly $V(CO)_6^{-1}$ is the molecule with the most multi-configurational character.

The CAS for ScF_6^{-3}, TiF_6^{-2}, and VF_6^{-1} are chosen to be the same, (10, 10), because it is an iso-electronic series. The MP2-srPBE NOOs for ScF_6^{-3} was close to 1.99 for the strongly occupied orbitals and close to 0.01 for the weakly occupied orbitals. For TiF_6^{-2} the NOOs are close to 1.99 and 0.012 to 0.017, and for VF_6^{-1} they are close to 1.98 and 0.020 to 0.037. The specific NOOs for the metal complexes using MP2–srPBE $\mu = 1.0$ are reported in Supplementary Information Table SI-16 – Table SI-21.

Information about how to retrieve the files used to run the calculations can be found in Supplementary Information.

IV. RESULTS

A. Comparisons to CC3 benchmark values

As an initial benchmark of the performance of HF–srDFT and CAS–srDFT for SSCCs, we compare to the CC3 benchmark values for 13 small molecules by Faber *et al.*[21] This benchmark set consists of small molecules with single reference character, and one therefore would expect the HF–srDFT and CAS-srDFT results to be very similar, and also similar to the KS-DFT values. As the question here is how well the various models agree with the reference CC3 values, we have chosen to report their *deviations* from the CC3 results with box plots, as defined in the figure captions. We also do not show box plots for the full isotropic values in order not to overload the figures, and because for reliable computational results the FC, SD, and PSO contributions must be reliable individually. The actual calculated SSCCs values and box plots for the total isotropic SSCCs can be found in Supplementary Information.

Before examining the results in more detail, we remark that it is known that KS-DFT struggles to predict SSCCs for couplings with fluorine[50,68]. The benchmark set has therefore been split into SSCCs not involving fluorine (25 SSCCs) and SSCCs involving fluorine (20 SSCCs) from 13 molecules. We report statistics for performance based on the mean absolute deviations (MADs) from the reference CC3 values for isotropic SSCCs. We summarize this analysis in Fig. 1 for the couplings not involving fluorine and in Fig. 2 for the couplings involving fluorine. All the values of the statistical errors for the FC, SD, and PSO terms can be seen in Supplementary Information Table SI-1 – Table SI-15. The deviations for the DSO expectation values are not reported as they are negligible compared to the FC, SD, and PSO errors.

In this benchmark set of molecules, the multi-configurational character is expected to be negligible, and indeed the results with CAS–srDFT are almost identical to those with HF–srDFT.

SSCCs for couplings not involving fluorine

First, we discuss the mean absolute deviations (MADs) for the couplings not involving fluorine reported in Fig. 1. Note the different scales for the FC results compared to SD and PSO. The SSCCs included here are four $^1J_{CO}$, two $^1J_{HO}$, two $^2J_{HH}$, two $^1J_{CN}$, five $^1J_{HC}$, one $^2J_{HN}$, three $^1J_{CC}$, two $^2J_{HC}$, one $^3J_{HH}$, one $^1J_{NO}$, and two $^2J_{HO}$. The dominant errors in these SSCCs clearly stem from the FC coupling, and we will therefore focus the discussion on the FC coupling. Some immediate conclusions can be extracted from the "Full $E^{[2]}$, FC" part of the figure. From "Full $E^{[2]}$" it can be seen that the three PBE-based models and the three LDA-based models are approximately of the same reliability and better than the CASSCF, which is without dynamical correlation. Looking closer, the three PBE methods are of the same quality and have a slightly smaller spread than the two srLDA methods, as can be seen both by the extensions of the boxes and the whiskers in Fig. 1. It can be noted that the improvement of the LDA model is much larger than the improvement of the PBE model when going to srLDA and srPBE models respectively. This is as expected since srLDA becomes a better approximation the more short-range the functional becomes (i.e. increasing μ), while PBE is already a good model at the KS-DFT level for these molecules. The last observation here is that the median values of the LDA calculations are superior compared to the PBE-based values, however, this is not a general trend which can be seen from the other results discussed below.

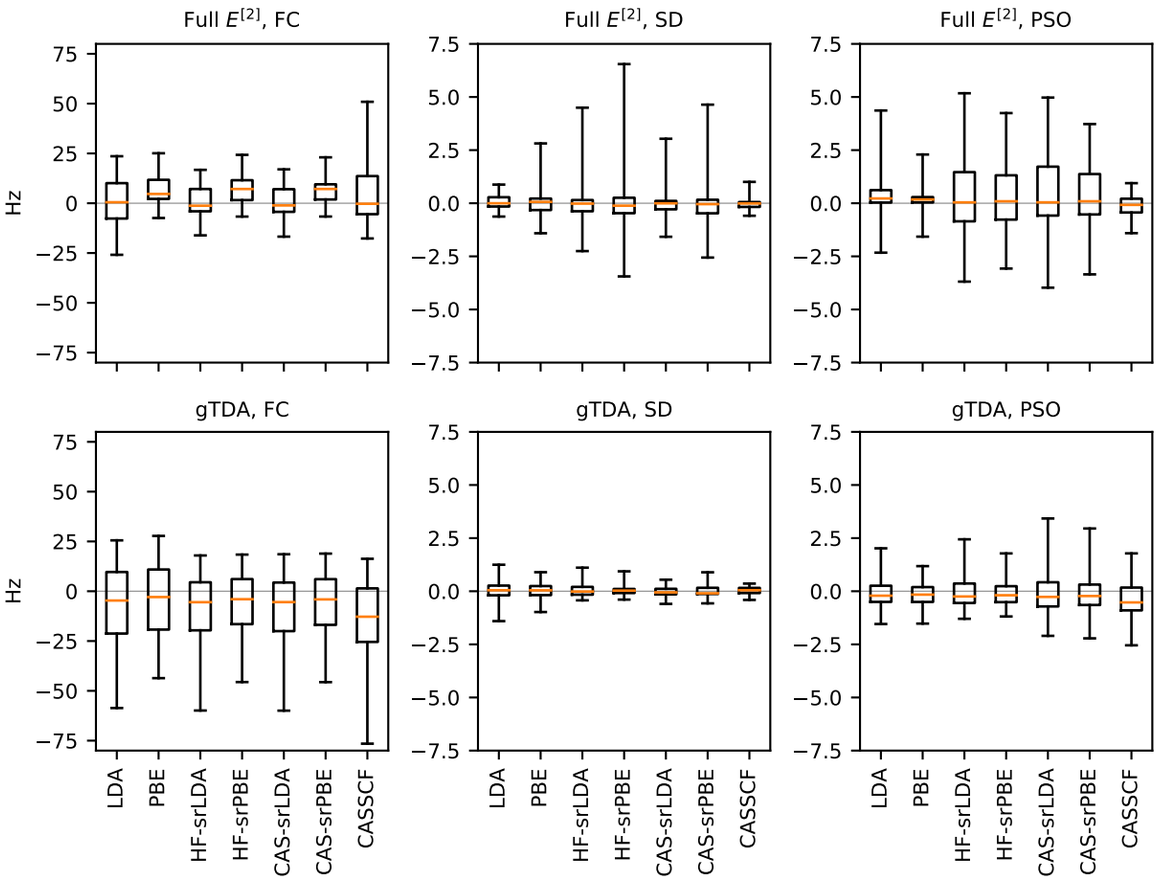

FIG. 1. MAD in Hz for the FC, SD, and PSO contributions with respect to the CC3 reference for all couplings not involving fluorine. Note the different scales for the FC results compared to SD and PSO. The colored line denotes the median value, the box is the middle 25% to the 75% quantile, and the whiskers denote max and min.

Let's now consider the lower half of Fig. 1, i.e. the gTDA part. Surprisingly, when looking at the triplet FC term, the full response ("Full $E^{[2]}$, FC") performs better than gTDA, i.e. than the Tamm-Dancoff approximation for the single determinant models and the generalized Tamm-Dancoff approximation for the multi-configurational models[25,69]. Similar findings of getting worse results when using TDA in the calculation of the FC term in the KS-DFT framework have been obtained by Cheng et al.[70]

In the remaining text, we write gTDA both for TDA and for gTDA. The gTDA is known to remove any triplet instabilities or near-instabilities, which often improves the calculation of triplet properties. However, comparing the box plots for FC using the "Full $E^{[2]}$" matrix with the box plots where the gTDA has been used, it is clear that the spread of "Full $E^{[2]}$, FC" is lower than that of "gTDA, FC" in Fig. 1. We have investigated this further for two cases with a large difference, $^2J_{\mathrm{HH}}$ for H_2O and $^1J_{\mathrm{CH}}$ for HCN. We calculated the triplet excitation energies and the transition moments for the FC operator with and without gTDA. The results show that the difference is mainly from a big change in the lowest FC transition moment and not from the change in triplet excitation energies. This indicates that for molecules not exhibiting near-triplet instabililities, the full calculations provide the most accurate transition moments.

On the other hand, the much smaller triplet response term, SD, does behave as expected, as can be seen in Fig. 1. We hypothesize that this is because the FC terms depend on the electronic wave function at the nucleus, while the SD terms depend more on the valence regions. The statistical errors in the last term, the singlet response PSO contribution, are the smallest for gTDA, this is also the opposite of what we expected beforehand.

In conclusion, for the molecules considered here the best model based on accuracy versus computational cost is the HF–srLDA model. To our knowledge, the performance of a long-range corrected LDA model has not been investigated previously.

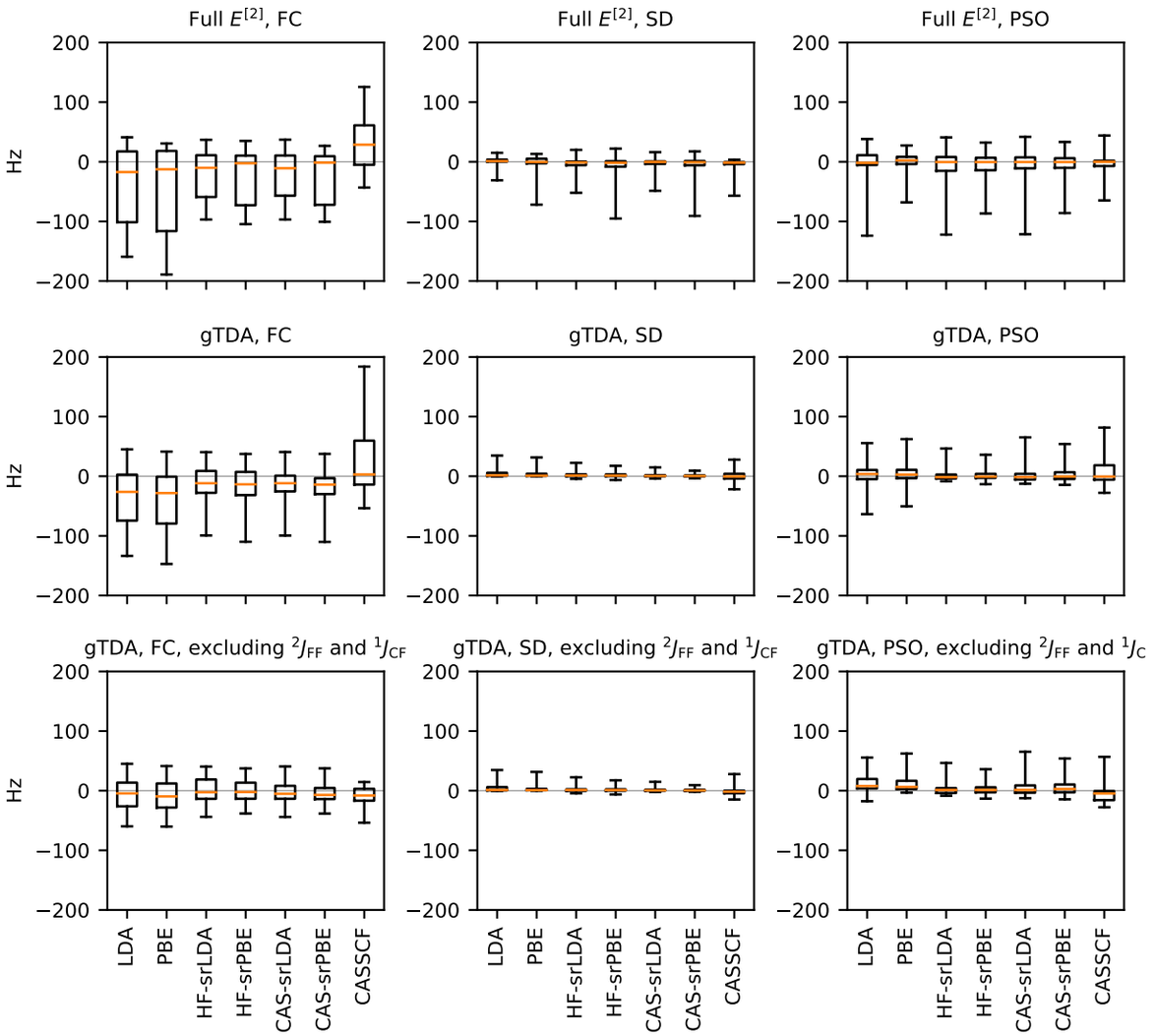

FIG. 2. MAD in Hz for the FC, SD, and PSO contributions with respect to the CC3 reference for all couplings involving fluorine. The first and second row excludes the $^2J_{FF}$ coupling from OF_2 as an outlier, due to the PSO term being more than 200 Hz different from the reference CC3 calculation, see SI Fig. 2. The bottom row is excluding $^2J_{FF}$ and $^1J_{CF}$ couplings. The colored line denotes the median value, the box is the middle 25% to the 75% quantile, and the whiskers denote max and min.

SSCCs for couplings involving fluorine

In the first two rows in Fig. 2 box plots of all SSCCs in the benchmark set involving fluorine can be seen. Note that the scales of all the plots are the same here. The SSCCs included here are two $^1J_{OF}$, two $^2J_{HF}$, two $^2J_{FF}$, five $^1J_{CF}$, one $^2J_{NF}$, two $^2J_{CF}$, one $^3J_{HF}$, one $^3J_{FF}$, one $^1J_{NF}$, and three $^2J_{OF}$. Again we first focus on the FC contribution. The median deviations are -21.45 Hz for LDA and -10.34 Hz for PBE. The spreads of LDA and PBE are comparable, ranging over more than 100 Hz for both of the methods. The spreads of HF–srLDA and HF–srPBE are also comparable, however, approximately reduced to half the size compared to LDA and PBE.

As for the couplings not involving fluorine discussed above, due to the lack of multi-configurational character in the benchmark set the quality of CAS–srDFT and HF–srDFT have spreads that are almost identical.

By inspecting the deviations for the individual spin-spin couplings we found that the couplings of the types $^2J_{FF}$, $^2J_{OF}$, and $^1J_{CF}$ are the only couplings with deviations above 20 Hz, see Fig. SI-2 in Supplementary Information. (The two most problematic cases are OF_2 and OHF.) From the third row in Fig. 2 it can be seen that exclusions of the problematic couplings $^2J_{FF}$ and $^1J_{CF}$ bring the statistical errors in the FC term to the same order of magnitude as for the couplings without fluorine in Fig. 1. This suggests that both KS-DFT and srDFT($\mu = 0.4$ bohr^{-1}) in particular have problems with $^2J_{FF}$ and $^1J_{CF}$ couplings.

Also here one notes that the cheaper srLDA is of the same quality as srPBE, and that "Full $E^{[2]}$" gives the best results for FC, while gTDA is best for SD and PSO. Here it should be noted that excluding ${}^2J_{\mathrm{FF}}$, and ${}^1J_{\mathrm{CF}}$ makes the FC contribution when using "Full $E^{[2]}$" and the FC contribution when using gTDA very comparable, see Figure SI-5.

B. Transition metal complexes with CO ligands, $M(CO)_y^{-z}$

In this subsection we investigate ${}^1J_{\mathrm{MC}}$ for the inorganic complexes $V(CO)_6^{-1}$, $Fe(CO)_5$ and $Co(CO)_4^{-1}$. The srDFT results presented here are for $\mu = 1.0$ bohr^{-1}, while the results above for organic molecules are for $\mu = 0.4$ bohr^{-1}, our standard μ value in our previous studies of the performance of srDFT for excitation energies and more. The choice of μ value will be discussed later. In Fig. 3 the calculated SSCCs for the seven studied DFT, HF–srDFT, CAS–srDFT, and CASSCF reference state models are reported in a bar chart, the numerical values can be found in Supplementary Information. For each of these wave function methods the SSCCs have been calculated using four choices for the linear response equations: 1) full response, 2) gTDA for both singlet and triplet contributions, 3) gTDA only for the singlet contributions, and 4) gTDA only for the triplet contributions.

We now proceed to analyze the results displayed in Fig. 3. First, it can be seen that the calculated SSCCs are very similar for LDA, PBE, HF–srLDA, and HF–srPBE for each of the four linear response choices. Furthermore, the calculated SSCCs are also very similar for CAS–srLDA and CAS–srPBE. Thus, as for the CC3 benchmark cases, the extra computational cost of the PBE/srPBE functionals compared to LDA/srLDA functionals is a waste of time. Second, by comparing "Full $E^{[2]}$" with "singlet gTDA" or, equivalently, by comparing "triplet gTDA" with "gTDA" we note that the effect of using singlet gTDA is visible in the figure for most of the seven models, but always unimportant. On the other hand, using gTDA on the triplet contributions to the SSCCs reduces the values of the calculated SSCCs by up to 22% for all of the srDFT models, and up to 31% for CASSCF. This is consistent with what was observed for the SSCCs in the CC3 benchmark that did not include F-couplings. For all three compounds, this makes the four single configuration DFT and HF–srDFT results somewhat less accurate with respect to the experimental SSCCs. For the three CAS–srDFT and CASSCF models there is no "winner", no choice which is always closest to experimental values.

C. Transition metal complexes with F ligands, MF_6^{-z}

In this subsection we investigate the model dependence of ${}^1J_{\mathrm{MF}}$ for the inorganic complexes ScF_6^{-3}, TiF_6^{-2}, and VF_6^{-1}. The srDFT results presented here are for $\mu = 1.0$ bohr^{-1}. In Fig. 4 the calculated SSCCs for the studied DFT, HF–srDFT, CAS–srDFT, and CASSCF methods are reported in a bar chart, the numerical values can be found in Supplementary Information. It is evident that (sr)LDA and (sr)PBE also perform very similarly for these three complexes.

For each method, the SSCCs are also here calculated in four ways; with and without gTDA for both triplet and singlet. The effect of singlet gTDA is enormous for the CAS–srDFT and CASSCF models for VF_6^{-1}, the calculated SSCCs change with approx. 200 Hz. The other two complexes behave as the $M(CO)_y^{-z}$ complexes; using gTDA on the singlet contributions to the SSCCs have only negligible effect, and using gTDA on the triplet contributions to the SSCCs reduces the absolute value of the calculated SSCCs.

It is striking that the calculated SSCCs exhibit a big change in the right direction towards the experimental values for HF–srDFT compared to DFT. It is also striking that it is necessary to go on to multi-configurational CAS–srDFT models to obtain calculated SSCCs close to experimental values. In comparison, for the couplings involving fluorine in the CC3 benchmark the HF–srDFT results were also much better than the DFT results but there qualitatively equal to the CAS–srDFT results, cf. Fig. 2. The DFT to HF–srDFT improvements for all couplings involving fluor can therefore be attributed to the range-separation of the functionals.

The need for CAS–srDFT to calculate SSCCs close to experimental values evidently means that it is essential to use a multi-configurational description to get useful values for metal-fluorine couplings. The numbers also show that the effects of using a multi-configurational description is much greater here than for the $M(CO)_y^{-z}$ complexes. However, the NOOs from MP2–srDFT reported in Sec. III for all six transition metal complexes are all so close to being 2 and 0 that we *a priori* expected multi-configurational effects to be similar for all six complexes. In fact, the NOO analysis shows that $V(CO)_6^{-1}$ is the most multi-configurational of the six compounds, so from that point of view, it was a surprise that a multi-configuration description is much more important for the metal-fluorine couplings.

Now we turn to another surprising result, the very model dependent SSCCs for VF_6^{-1}. The four ways to solve the response equations give so different results for all models that one would think they were calculations on different molecules if one didn't know the truth. For the other five metal complexes, the SSCCs are dominated by the FC term, however, for VF_6^{-1} both the FC term and the PSO term are roughly of the same magnitude, $\sim$300 to $\sim$500 Hz, but with different sign. This fact means that we can use this complex to get a deeper insight in the performance of the different models considered here. Fig. 4 shows that *only* the two CAS–srDFT with singlet gTDA models give a good prediction of the experimental value, all the other calculations are qualitatively wrong. Once more, CAS–srPBE gives approximately the same values as CAS–srLDA.

Even though the HF–srDFT to CAS–srDFT improvements are particularly spectacular for VF_6^{-1}, the results do show a big effect of using CAS–srDFT instead of HF–srDFT for all three fluorine compounds. Considering that none of the three ground states are particularly multi-configurational, the effect must originate in the calculations of the linear response vectors. This view is also supported by the big differences in the

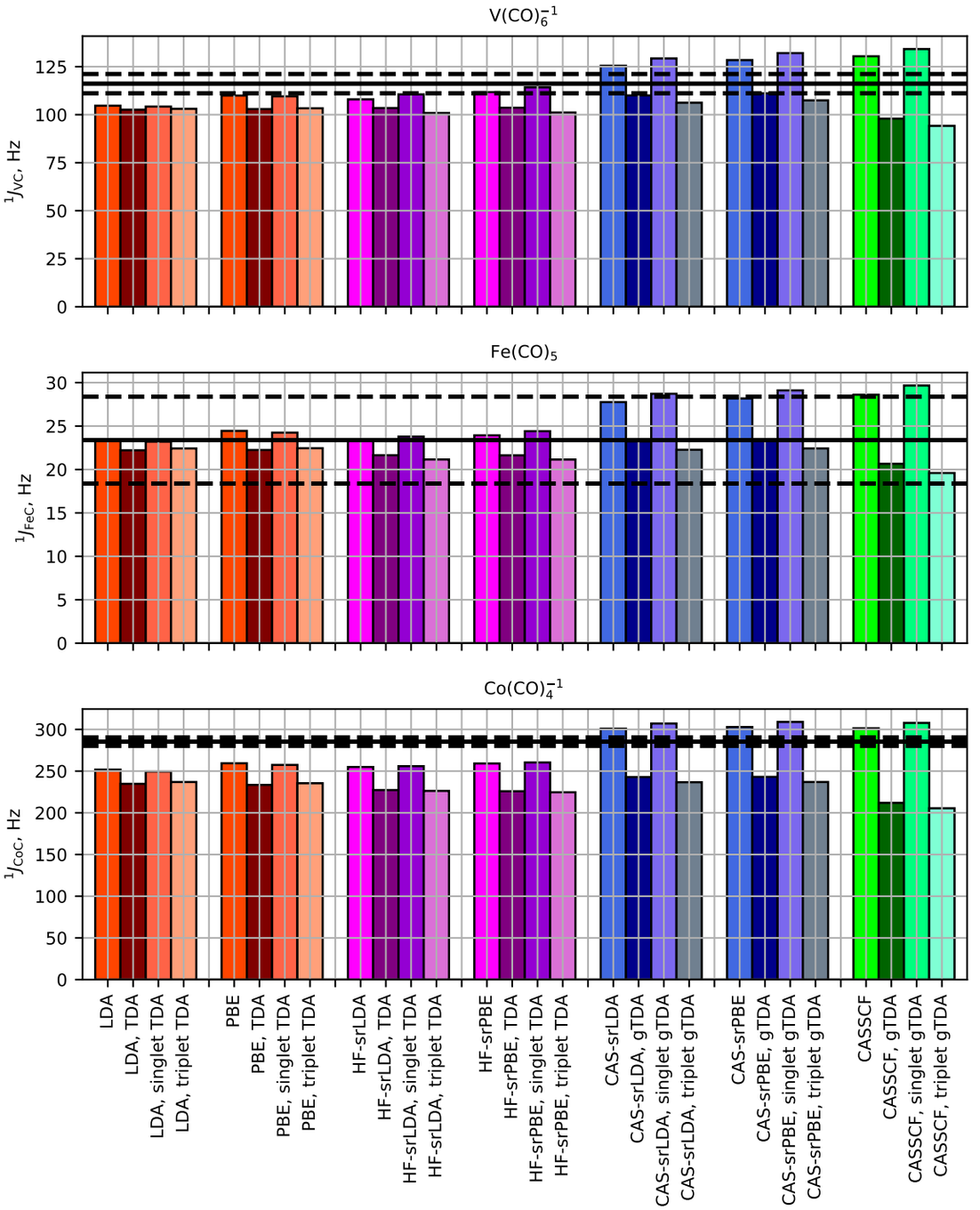

FIG. 3. Calculated SSCCs for the M(CO)$_y^{-z}$ complexes. All the srDFT calculations are with $\mu = 1.0$ bohr^{-1}. The black dashed lines is the reference coupling ± 5 Hz. For each method four results are reported: "Full $E^{[2]}$", full gTDA, only gTDA in singlet response, and only gTDA in triplet response.

calculated SSCCs for the four linear response methods. We remark that the orbitals we chose on the basis of MP2-srDFT NOOs correspond to including the d-shell and their correlating orbitals in the CAS, and these results thus indicate that it is important to do this to get reliable values.

Next, we turn to a discussion of the differences between the four models for the response solutions. The VF_6^{-1} results show that singlet gTDA can change the sign of the SSCCs

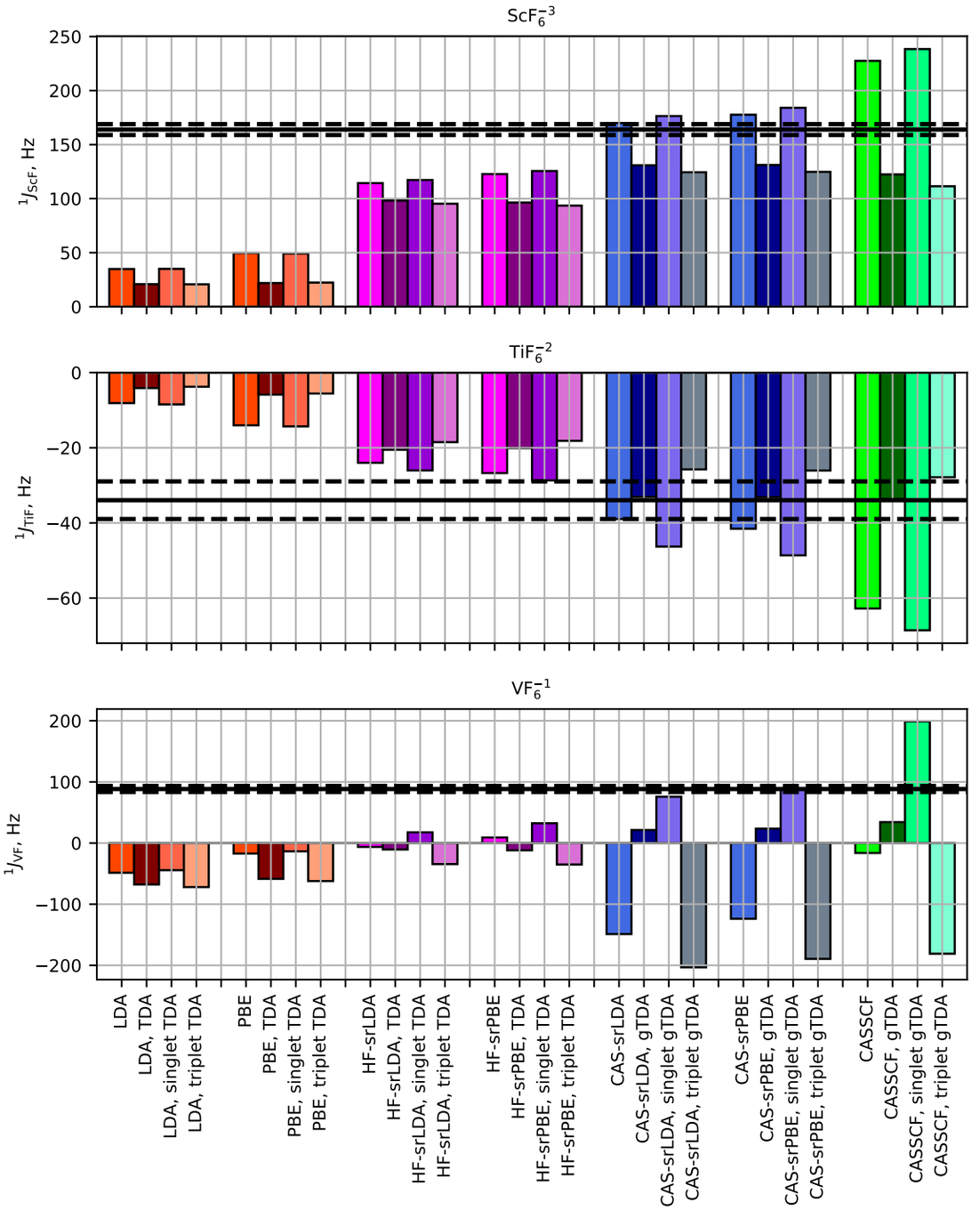

FIG. 4. Calculated SSCCs for the MF_6^{-z} complexes. All the srDFT calculations are with $\mu = 1.0$ bohr^{-1}. The black dashed lines is the reference coupling ± 5 Hz. For each method four results are reported: full $E^{[2]}$, full gTDA, only gTDA in singlet response, and only gTDA in triplet response.

compared to the full response, that is, it leads to a big change in the singlet PSO contribution. For the other molecules, the effect of using singlet gTDA is small, reflecting that the FC term dominates the PSO term for them. The triplet gTDA gives a negative contribution of approximately the same size as for the other metal complexes. This leads to completely wrong results for VF_6^{-1}. For the other five complexes, one cannot conclude from the results if with or without triplet

gTDA is best. It is outside the scope of this paper to investigate why singlet gTDA is so much better than full singlet response, this will be interesting to analyze in future work.

Finally, the measured SSCCs are in aquatic solution while the calculations are for vacuum, so this is also a source of deviation to the experimental values. To test this we have performed LDA/PCM calculations on the MF_6^{-z} molecules with water as solvent. The SSCCs from LDA/PCM only deviated up to 2.3 Hz from the LDA calculations, so we believe solvent effects are not important for the conclusions, see Table SI-26 in Supplementary Information.

D. Comments on the choice of μ value

We end this section with a discussion of why we ended up using $\mu = 1.0$ bohr^{-1} for the six metal complexes instead of $\mu = 0.4$ bohr^{-1}, our tested choice in previous works.[25,29,71] First we note that a reasonable measure for the extent of the short-range region is $r^{sr} = \mu^{-1}$ for the range-separation defined in Eq. (8) and used in this work, corresponding to 2.5 bohr for $\mu = 0.4$ bohr^{-1} and 1.0 bohr for $\mu = 1.0$ bohr^{-1}.

In Figs. SI-3 and SI-4 in Supplementary Information the calculated SSCCs for the six metal complexes are reported for both $\mu = 0.4$ bohr^{-1} and $\mu = 1.0$ bohr^{-1}. A general observation for all six metal complexes is that the predicted SSCCs by HF-srDFT($\mu = 0.4$), HF-srDFT($\mu = 1.0$), and CAS-srDFT($\mu = 0.4$) are very close. Only CAS-srDFT($\mu = 1.0$) is substantially different from these three, and its combination with singlet gTDA linear response is the *only* model that provides SSCCs close to the experimental results for all six complexes.

The comparisons in this subsection show that there are non-dynamical correlation effects for the transition metals in the r_{12} range 1 to 2.5 bohr, correlation effects which are clearly not described by the srDFT functionals. If these correlation effects had been beyond 2.5 bohr, then CAS-srDFT($\mu = 0.4$) results should have been different from HF-srDFT($\mu = 0.4$) results. We did test $\mu = 0.8$ for two cases and found that it did not change the general picture. In future work, we will investigate in more detail what the optimal μ-value is for transition metal complexes, and why. It is outside the scope of this work.

V. CONCLUSIONS

We have extended the HF–srDFT and MC–srDFT models to calculations of indirect spin-spin coupling constants (SSCCs), and we have investigated the performance of these new computational alternatives. We compared to CC3 values for a benchmark set of thirteen small molecules[21] and to experimental SSCCs for six transition metal complexes. Based on all the calculated SSCCs we can draw some general conclusions. The fact that these observations are valid for the different types of molecules studied here suggests that the conclusions could very well be correct for other types of molecules, and therefore that an MC–srDFT model for SSCCs could become a standard choice for a reliable computational prediction of SSCCs at a relatively low computational cost. The computational cost is equal to the combined cost of a KS–DFT calculation and an MCSCF calculation with a smaller active space than usual for CASSCF.

First, the SSCCs from the computationally cheaper srLDA xc-functional are as good as those from the srPBE xc-functional, and we, therefore, advocate to use MC–srLDA in production calculations. In fact, the LDA accuracy is in most cases also close to the accuracy with PBE. We did see the same performance of srLDA vs. srPBE recently for triplet excitation energies,[25] this can explain that we see the same for FC if we interpret the FC calculations in a sum-over-states formalism.

Second, the best results have been obtained with singlet gTDA and without triplet gTDA, this combination gave always reasonable results (gTDA is an abbreviation for the generalized Tamm-Dancoff approximation). For one molecule, VF_6^{-1}, all other combinations gave completely wrong predictions, cf. Fig. 4. Both of these choices were surprising to us. It is well-known that triplet gTDA is needed to get good predictions of low-lying triplet excitation energies because of the common case of near-triplet or triplet instabilities, as we also have found for triplet excitation energies with MC–srDFT.[25] The most logical explanation is that the low-lying triplet excitations have a negligible contribution to FC, while the excitation energies important for FC are improved with a full response calculation. It is even more surprising that the singlet gTDA is essential to obtain reliable PSO contributions. It shall be interesting to investigate further why in future work.

Next, we summarize the more specific conclusions for the four classes of molecules tested here. The small molecules in the CC3 benchmark set for SSCCs[21] all have single reference character, i.e. no significant non-dynamical correlation. One would therefore expect HF–srDFT values to be close to the CAS–srDFT values, and this was confirmed by the calculations cf. Figs. 1 and 2. It is well-known that KS–DFT struggles to predict couplings with fluorine, and we, therefore, divided the benchmark set into two sets, one with the 25 SSCCs not involving fluorine and one with the remaining 20 SSCCs involving fluorine. For SSCCs not involving fluorine the quality of the calculated SSCCs with HF–srDFT was similar to that of conventional KS-DFT. For SSCCs involving fluorine HF–srDFT reduced the errors compared to conventional KS-DFT. A closer analysis revealed that not all couplings involving fluorine are equally difficult to calculate, the statistical errors for $^1J_{OF}$,$^2J_{FF}$, and $^1J_{CF}$ were much greater than for $^2J_{HF}$, $^2J_{NF}$, $^2J_{CF}$, $^3J_{HF}$, $^3J_{FF}$, $^1J_{NF}$, and $^2J_{OF}$.

We have also investigated the performance of CAS–srDFT for metal to ligand SSCCs for six inorganic transition metal (TM) complexes. We found for the first time that our hitherto standard choice of $\mu = 0.4$ bohr^{-1} failed. Only with the much larger value $\mu = 1.0$ bohr^{-1} did we obtain good predictions for all six cases, in particular for fluorine ligands. As explained in subsection IV D, this implies that the metal centers exhibit significant non-dynamical correlation for inter-electronic distances in the range 1.0 to 2.5 bohr that cannot be described by the srLDA or srPBE functionals. We attribute this to correlation of the d-electrons, this is corroborated by

the observation that at least a double set of d-orbitals should be in the active space to get good values.

Zooming in, for the J_{MC} couplings in three $M(CO)_6$ complexes all investigated methods appear to perform equally well compared to the experimental measurements, in particular, the long-range corrected HF–srDFT predictions are close to the KS–DFT values. This is definitely not the case for the J_{MF} couplings in three MF_6 transition metal complexes. As for the CC3 benchmark, the best results are obtained by using gTDA for the singlet PSO and not using gTDA for the triplet FC. For the most demanding case, VF_6^{-1}, the CAS–srLDA and CAS–srPBE with singlet generalized Tamm-Dancoff approximation (gTDA) are spot on the experimental result, all other methods are not even close. This case turned out to be especially useful to investigate the quality of models because the FC and PSO terms here have different signs. Also for the other two J_{MF} couplings, the only good predictions are from CAS–srDFT, however here the effect of singlet gTDA or not is small, this is because the PSO term is much smaller than the FC term for them. Qualitatively the long-range correction in HF–srDFT reduce the errors by a factor 2; the non-dynamical correlation in CAS–srDFT is essential to get rid of the remaining errors.

Based on the results of this paper we propose the following computational recipe for SSCCs with MC–srDFT after the definition of molecular geometry and basis set:

- Use srLDA functional
- Use $\mu = 1.0$ bohr^{-1} for transition metal complexes, use $\mu = 0.4$ bohr^{-1} for organic molecules.
- Use MP2–srLDA natural orbital occupation numbers to select active space in CAS–srLDA or HF–srLDA.
- Use singlet gTDA for the calculation of PSO contributions.
- Do not use triplet gTDA for the FC contributions, except possibly for SSCCs not involving fluorine for organic molecules. Triplet gTDA does improve the SD contributions, but it is usually unimportant.
- SSCC for transition metal complexes might need a larger CAS than suggested by MP2–srLDA orbitals, because our calculations showed that correlation of the whole d-shell could be important to get reliable values.

Finally, we note that we have used a development version of the DALTON2018 code[37] for all the calculations presented here. Our new code for MC-srDFT SSCCs calculations has been released in DALTON2020[27] and is available for download. See Supplementary Information for information about molecular coordinates and Dalton input files used in this work.

SUPPLEMENTARY MATERIAL

See supplementary material for more statistical details of the SSCC benchmark set, MP2–srPBE NOO, calculated SSCC for transition metal complexes using $\mu = 0.4$ bohr^{-1}, and PCM effects on the SSCC of XF_6 complexes using LDA.

ACKNOWLEDGMENTS

We thank the Danish e-infrastructure Cooperation (DeiC) and University of Southern Denmark for computational resources for this work.

DATA AVAILABILITY STATEMENT

The data that support the findings of this study are openly available in "MC–srDFT spin-spin coupling constants input files for Dalton" at http://doi.org/10.5281/zenodo.4899982.

[1] T. Helgaker, M. Jaszuński, and K. Ruud, "Ab initio methods for the calculation of NMR shielding and indirect spin-spin coupling constants," Chemical Reviews **99**, 293–352 (1999).
[2] J. Vaara, "Theory and computation of nuclear magnetic resonance parameters," Physical Chemistry Chemical Physics **9**, 5399 (2007).
[3] M. W. Lodewyk, M. R. Siebert, and D. J. Tantillo, "Computational prediction of ^{1}H and ^{13}C chemical shifts: A useful tool for natural product, mechanistic, and synthetic organic chemistry," Chemical Reviews **112**, 1839–1862 (2011).
[4] N. F. Ramsey, "Electron coupled interactions between nuclear spins in molecules," Phys. Rev. **91**, 303–307 (1953).
[5] T. Helgaker, M. Watson, and N. C. Handy, "Analytical calculation of nuclear magnetic resonance indirect spin-spin coupling constants at the generalized gradient approximation and hybrid levels of density-functional theory," The Journal of Chemical Physics **113**, 9402–9409 (2000).
[6] J. Autschbach and T. Ziegler, "Nuclear spin-spin coupling constants from regular approximate relativistic density functional calculations. I. Formalism and scalar relativistic results for heavy metal compounds," The Journal of Chemical Physics **113**, 936–947 (2000).
[7] V. Sychrovský, J. Gräfenstein, and D. Cremer, "Nuclear magnetic resonance spin-spin coupling constants from coupled perturbed density functional theory," The Journal of Chemical Physics **113**, 3530–3547 (2000).
[8] V. Barone, J. E. Peralta, R. H. Contreras, and J. P. Snyder, "DFT calculation of NMR J_{FF} spin-spin coupling constants in fluorinated pyridines," The Journal of Physical Chemistry A **106**, 5607–5612 (2002).
[9] A. D. Becke, "Perspective: Fifty years of density-functional theory in chemical physics," The Journal of Chemical Physics **140**, 18A301 (2014).
[10] V. G. Malkin, O. L. Malkina, and D. R. Salahub, "Calculation of spin-spin coupling constants using density functional theory," Chemical Physics Letters **221**, 91–99 (1994).
[11] R. M. Dickson and T. Ziegler, "NMR spin-spin coupling constants from density functional theory with Slater-type basis functions," The Journal of Physical Chemistry **100**, 5286–5290 (1996).
[12] J. Geertsen and J. Oddershede, "Second-order polarization propagator calculations of indirect nuclear spin-spin coupling tensors in the water molecule," Chemical Physics **90**, 301–311 (1984).
[13] J. Geertsen and J. Oddershede, "Higher RPA and second-order polarization propagator calculations of coupling constants in acetylene," Chemical Physics **104**, 67–72 (1986).
[14] T. Enevoldsen, J. Oddershede, and S. P. A. Sauer, "Correlated calculations of indirect nuclear spin-spin coupling constants using second-order polarization propagator approximations: SOPPA and SOPPA(CCSD)," Theoretical Chemistry Accounts: Theory, Computation, and Modeling (Theoretica Chimica Acta) **100**, 275–284 (1998).
[15] H. Kjær, S. P. A. Sauer, and J. Kongsted, "Benchmarking NMR indirect nuclear spin-spin coupling constants: SOPPA, SOPPA(CC2), and SOPPA(CCSD) versus CCSD," The Journal of Chemical Physics **133**, 144106 (2010).
[16] I. L. Rusakova, L. B. Krivdin, Y. Y. Rusakov, and A. B. Trofimov, "Algebraic-diagrammatic construction polarization propagator approach to indirect nuclear spin–spin coupling constants," The Journal of Chemical Physics **137**, 044119 (2012).
[17] H. Sekino and R. J. Bartlett, "Nuclear spin-spin coupling constants evaluated using many body methods," The Journal of Chemical Physics **85**, 3945–3949 (1986).

[18]S. A. Perera, H. Sekino, and R. J. Bartlett, "Coupled-cluster calculations of indirect nuclear coupling constants: The importance of non-fermi contact contributions," The Journal of Chemical Physics **101**, 2186–2191 (1994).
[19]S. A. Perera, M. Nooijen, and R. J. Bartlett, "Electron correlation effects on the theoretical calculation of nuclear magnetic resonance spin-spin coupling constants," The Journal of Chemical Physics **104**, 3290–3305 (1996).
[20]A. A. Auer and J. Gauss, "Triple excitation effects in coupled-cluster calculations of indirect spin-spin coupling constants," The Journal of Chemical Physics **115**, 1619–1622 (2001).
[21]R. Faber, S. P. A. Sauer, and J. Gauss, "Importance of triples contributions to NMR spin-spin coupling constants computed at the CC3 and CCSDT levels," Journal of Chemical Theory and Computation **13**, 696–709 (2017).
[22]O. Vahtras, H. Ågren, P. Jørgensen, H. Jørgen Aa. Jensen, S. B. Padkjær, and T. Helgaker, "Indirect nuclear spin–spin coupling constants from multiconfiguration linear response theory," J. Chem. Phys. **96**, 6120–6125 (1992).
[23]A. Barszczewicz, T. Helgaker, M. Jaszuński, P. Jørgensen, and K. Ruud, "Multiconfigurational self-consistent field calculations of nuclear magnetic resonance indirect spin-spin coupling constants," The Journal of Chemical Physics **101**, 6822–6828 (1994).
[24]M. Hubert, E. D. Hedegård, and H. J. Aa. Jensen, "Investigation of Multiconfigurational Short-Range Density Functional Theory for Electronic Excitations in Organic Molecules," J. Chem. Theory Comput. **12**, 2203–2213 (2016).
[25]E. R. Kjellgren, E. D. Hedegård, and H. J. A. Jensen, "Triplet excitation energies from multiconfigurational short-range density-functional theory response calculations," The Journal of Chemical Physics **151**, 124113 (2019).
[26]K. Aidas, C. Angeli, K. L. Bak, V. Bakken, R. Bast, L. Boman, O. Christiansen, R. Cimiraglia, S. Coriani, P. Dahle, E. K. Dalskov, U. Ekström, T. Enevoldsen, J. J. Eriksen, P. Ettenhuber, B. Fernández, L. Ferrighi, H. Fliegl, L. Frediani, K. Hald, A. Halkier, C. Hättig, H. Heiberg, T. Helgaker, A. C. Hennum, H. Hettema, E. Hjertenæs, S. Høst, I.-M. Høyvik, M. F. Iozzi, B. Jansík, H. J. Aa. Jensen, D. Jonsson, P. Jørgensen, J. Kauczor, S. Kirpekar, T. Kjærgaard, W. Klopper, S. Knecht, R. Kobayashi, H. Koch, J. Kongsted, A. Krapp, K. Kristensen, A. Ligabue, O. B. Lutnæs, J. I. Melo, K. V. Mikkelsen, R. H. Myhre, C. Neiss, C. B. Nielsen, P. Norman, J. Olsen, J. M. H. Olsen, A. Osted, M. J. Packer, F. Pawlowski, T. B. Pedersen, P. F. Provasi, S. Reine, Z. Rinkevicius, T. A. Ruden, K. Ruud, V. V. Rybkin, P. Sałek, C. C. M. Samson, A. S. de Merás, T. Saue, S. P. A. Sauer, B. Schimmelpfennig, K. Sneskov, A. H. Steindal, K. O. Sylvester-Hvid, P. R. Taylor, A. M. Teale, E. I. Tellgren, D. P. Tew, A. J. Thorvaldsen, L. Thøgersen, O. Vahtras, M. A. Watson, D. J. D. Wilson, M. Ziolkowski, and H. Ågren, "The Dalton quantum chemistry program system," Wiley Interdisciplinary Reviews: Computational Molecular Science **4**, 269–284 (2013).
[27]"DALTON, a molecular electronic structure program, Release Dalton2020, see `http://daltonprogram.org`," (2020).
[28]A. Abragam, *The Principles of Nuclear Magnetism* (Oxford University Press, 1983).
[29]E. Fromager, J. Toulouse, and H. J. Aa. Jensen, "On the universality of the long-/short range separation in multiconfigurational Density-Functional Theory," J. Chem. Phys. **126**, 074111 (2007).
[30]E. Fromager, S. Knecht, and H. J. Aa. Jensen, "Multi-Configuration Time-Dependent Density-Functional Theory based on range separation," J. Chem. Phys. **138**, 084101 (2013).
[31]E. D. Hedegård, J. M. H. Olsen, S. Knecht, J. Kongsted, and H. J. Aa. Jensen, "Polarizable embedding with a multiconfiguration short-range density functional theory linear response method," J. Chem. Phys. **114**, 1102–1107 (2015).
[32]E. D. Hedegård, J. Toulouse, and H. J. Aa. Jensen, "Multiconfigurational short-range density-functional theory for open-shell systems," J. Chem. Phys **148**, 214103 (2018).
[33]T. Saue and T. Helgaker, "Four-component relativistic Kohn-Sham theory," Journal of Computational Chemistry **23**, 814–823 (2002).
[34]P. Sałek, O. Vahtras, T. Helgaker, and H. Ågren, "Density-functional theory of linear and nonlinear time-dependent molecular properties," The Journal of Chemical Physics **117**, 9630–9645 (2002).
[35]J. Olsen and P. Jørgensen, "Linear and non-linear response functions for an exact state and for an MCSCF state," J. Chem. Phys. **82**, 3235–3264 (1985).
[36]J. Olsen, D. L. Yeager, and P. Jørgensen, "Triplet excitation properties in large scale multiconfiguration linear response calculations," J. Chem. Phys **91**, 381–388 (1989).
[37]"DALTON, a molecular electronic structure program, Release Dalton2018, see `http://daltonprogram.org`," (2018).
[38]S. Paziani, S. Moroni, P. Gori-Giorgi, and G. B. Bachelet, "Local-spin-density functional for multideterminant density functional theory," Phys. Rev. B **73**, 155111 (2006).
[39]E. Goll, H.-J. Werner, and H. Stoll, "A short-range gradient-corrected density functional in long-range coupled-cluster calculations for rare gas dimers," Phys. Chem. Chem. Phys. **7**, 3917–3923 (2005).
[40]E. Goll, H.-J. Werner, H. Stoll, T. Leininger, P. Gori-Giorgi, and A. Savin, "A short-range gradient-corrected spin density functional in combination with long-range coupled-cluster methods: Application to alkali-metal rare-gas dimers," Chem. Phys. **329**, 276–282 (2006).
[41]S. H. Vosko, L. Wilk, and M. Nusair, "Accurate spin-dependent electron liquid correlation energies for local spin density calculations: a critical analysis," Can. J. Phys. **58**, 1200–1211 (1980).
[42]P. Hohenberg and W. Kohn, "Inhomogeneous electron gas," Phys. Rev. **136**, B864–B871 (1964).
[43]W. Kohn and L. J. Sham, "Self-consistent equations including exchange and correlation effects," Phys. Rev. **140**, A1133–A1138 (1965).
[44]J. C. Slater and J. C. Phillips, "Quantum theory of molecules and solids vol. 4: The self-consistent field for molecules and solids," Physics Today **27**, 49–50 (1974).
[45]J. P. Perdew, K. Burke, and M. Ernzerhof, "Generalized Gradient Approximation made simple," Phys. Rev. Lett. **77**, 3865–3868 (1996).
[46]U. Benedikt, A. A. Auer, and F. Jensen, "Optimization of augmentation functions for correlated calculations of spin-spin coupling constants and related properties," J. Chem. Phys. **129**, 064111 (2008).
[47]R. A. Kendall, T. H. Dunning, and R. J. Harrison, "Electron affinities of the first-row atoms revisited. Systematic basis sets and wave functions," J. Chem. Phys. **96**, 6796–6806 (1992).
[48]R. Faber and S. P. A. Sauer, "On the convergence of the ccJ-pVXZ and pcJ-n basis sets in CCSD calculations of nuclear spin–spin coupling constants: some difficult cases," Theoretical Chemistry Accounts **137** (2018), 10.1007/s00214-018-2217-0.
[49]J. Khandogin and T. Ziegler, "A density functional study of nuclear magnetic resonance spin-spin coupling constants in transition-metal systems," Spectrochimica Acta Part A: Molecular and Biomolecular Spectroscopy **55**, 607–624 (1999).
[50]V. Barone, P. F. Provasi, J. E. Peralta, J. P. Snyder, S. P. A. Sauer, and R. H. Contreras, "Substituent effects on scalar $^2J(^{19}\mathrm{F},^{19}\mathrm{F})$ and $^3J(^{19}\mathrm{F},^{19}\mathrm{F})$ NMR couplings: A comparison of SOPPA and DFT methods," J. Phys. Chem. A **107**, 4748–4754 (2003).
[51]E. D. Hedegård, J. Kongsted, and S. P. A. Sauer, "Optimized basis sets for calculation of electron paramagnetic resonance hyperfine coupling constants: aug-cc-pVTZ-J for the 3d atoms Sc-Zn," J. Chem. Theory Comput. **7**, 4077–4087 (2011).
[52]P. F. Provasi, G. A. Aucar, and S. P. A. Sauer, "The effect of lone pairs and electronegativity on the indirect nuclear spin-spin coupling constants in CH_2X (X=CH_2, NH, O, S):ab initiocalculations using optimized contracted basis sets," J. Chem. Phys. **115**, 1324–1334 (2001).
[53]P. F. Provasi and S. P. A. Sauer, "Optimized basis sets for the calculation of indirect nuclear spin-spin coupling constants involving the atoms B, Al, Si, P, and Cl," J. Chem. Phys. **133**, 054308 (2010).
[54]B. Mann, ^{13}*C NMR Data for Organometallic Compounds (Organometallic chemistry)* (Academic Pr, 1982).
[55]M. J. Buckingham, G. E. Hawkes, and J. R. Thornback, "The ^{99}Tc and ^{17}O nuclear magnetic spectra of TcO_4^- –the first detailed report of a ^{99}Tc resonance," Inorganica Chimica Acta **56**, L41–L42 (1981).
[56]N. Hao, B. G. Sayer, G. Dénès, D. G. Bickley, C. Detellier, and M. J. McGlinchey, "Titanium-47 and -49 nuclear magnetic resonance spectroscopy: Chemical applications," Journal of Magnetic Resonance (1969) **50**, 50–63 (1982).
[57]N. Hao, M. J. McGlinchey, B. G. Sayer, and G. J. Schrobilgen, "A ^{61}Ni NMR study of some d^{10} nickel complexes," Journal of Magnetic Resonance (1969) **46**, 158–162 (1982).
[58]D. Rehder, H.-C. Bechthold, A. Keçeci, H. Schmidt, and M. Siewing, "A comparative study of metal shielding in low valent vanadium, niobium

and manganese complexes," Zeitschrift für Naturforschung B **37**, 631–645 (1982).
[59]J. Banck and A. Schwenk, "183-Tungsten NMR studies," Zeitschrift für Physik B Condensed Matter and Quanta **20**, 75–80 (1975).
[60]G. L. J.T. Bailey, R.J. Clark, "Molybdenum nuclear magnetic resonance studies of trifluorophosphine complexes," Inorg. Chem. **21**, 2086 (1982).
[61]E. A. C. Lucken, K. Noack, and D. F. Williams, "59co nuclear magnetic resonance of organo-cobalt compounds," Journal of the Chemical Society A: Inorganic, Physical, Theoretical , 148 (1967).
[62]M. L. Martin, "B. e. mann and b. f. taylor.13c NMR data for organometallic compounds. academic press, london, 1981. pp. 326." Organic Magnetic Resonance **19**, vi–vi (1982).
[63]G. M. Bodner and L. J. Todd, "Fourier transform carbon-13 nuclear magnetic resonance study of transition metal carbonyl complexes," Inorganic Chemistry **13**, 1335–1338 (1974).
[64]B. P. Pritchard, D. Altarawy, B. Didier, T. D. Gibsom, and T. L. Windus, "A new basis set exchange: An open, up-to-date resource for the molecular sciences community," J. Chem. Inf. Model. **59**, 4814–4820 (2019).
[65]D. Feller, "The role of databases in support of computational chemistry calculations," J. Comput. Chem. **17**, 1571–1586 (1996).
[66]K. L. Schuchardt, B. T. Didier, T. Elsethagen, L. Sun, V. Gurumoorthi, J. Chase, J. Li, and T. L. Windus, "Basis set exchange: A community database for computational sciences," J. Chem. Inf. Model. **47**, 1045–1052 (2007).
[67]H. J. Aa. Jensen, P. Jørgensen, H. Ågren, and J. Olsen, "Second-order møller–plesset perturbation theory as a configuration and orbital generator in multiconfiguration self-consistent field calculations," J. Chem. Phys. **88**, 3834–3839 (1988).
[68]J. G. de la Vega and J. S. Fabián, "Assessment of DFT functionals with fluorine–fluorine coupling constants," Molecular Physics **113**, 1924–1936 (2015).
[69]B. Helmich-Paris, "CASSCF linear response calculations for large open-shell molecules," The Journal of Chemical Physics **150**, 174121 (2019).
[70]C. Y. Cheng, M. S. Ryley, M. J. Peach, D. J. Tozer, T. Helgaker, and A. M. Teale, "Molecular properties in the tamm-dancoff approximation: indirect nuclear spin-spin coupling constants," Molecular Physics **113**, 1937–1951 (2015).
[71]M. Hubert, H. J. Aa. Jensen, and E. D. Hedegård, "Excitation Spectra of Nucleobases with Multiconfigurational Density Functional Theory," J. Phys. Chem. A **120**, 36–43 (2016).

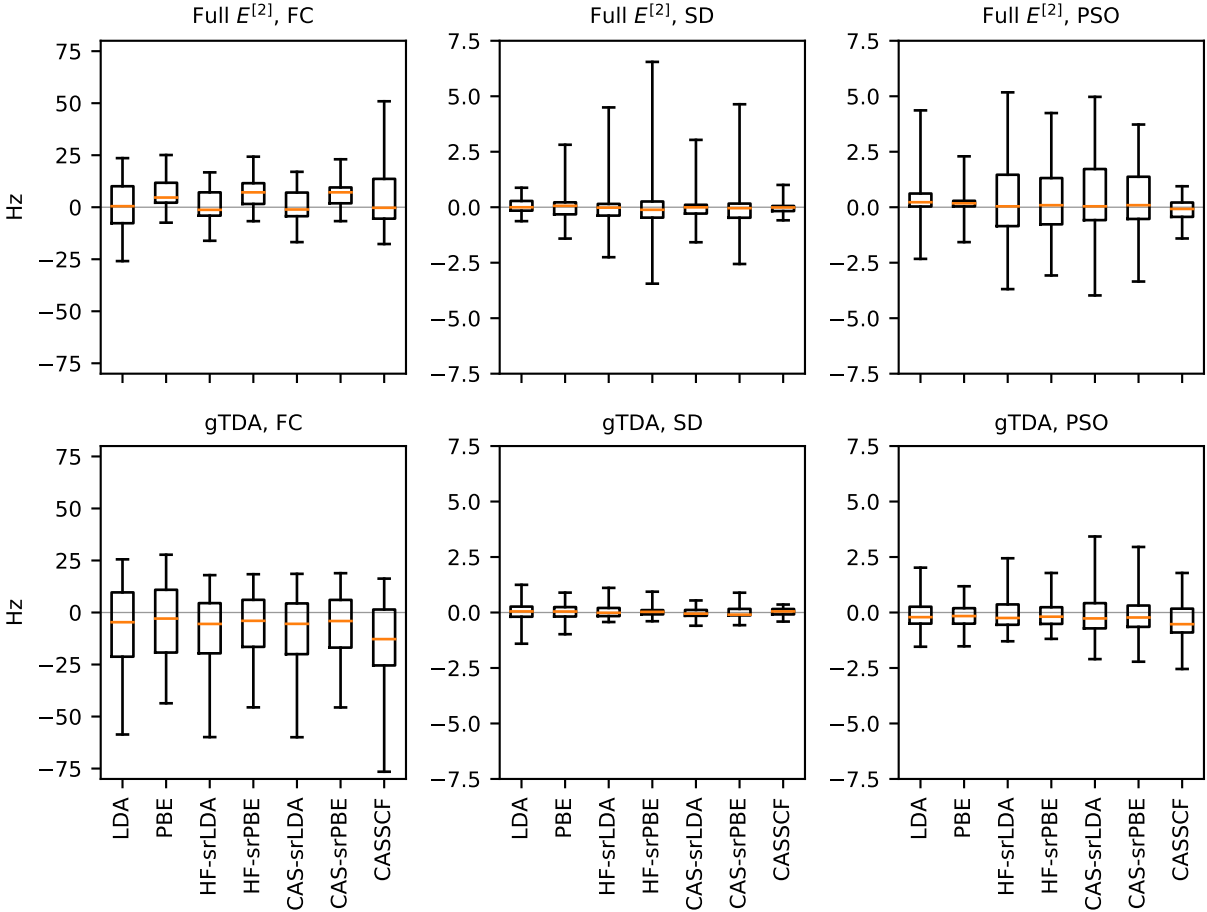
Full $E^{[2]}$, FC
Full $E^{[2]}$, SD
Full $E^{[2]}$, PSO
gTDA, FC
gTDA, SD
gTDA, PSO
Hz
75
50
25
0
−25
−50
−75
7.5
5.0
2.5
0.0
−2.5
−5.0
−7.5
LDA
PBE
HF-srLDA
HF-srPBE
CAS-srLDA
CAS-srPBE
CASSCF

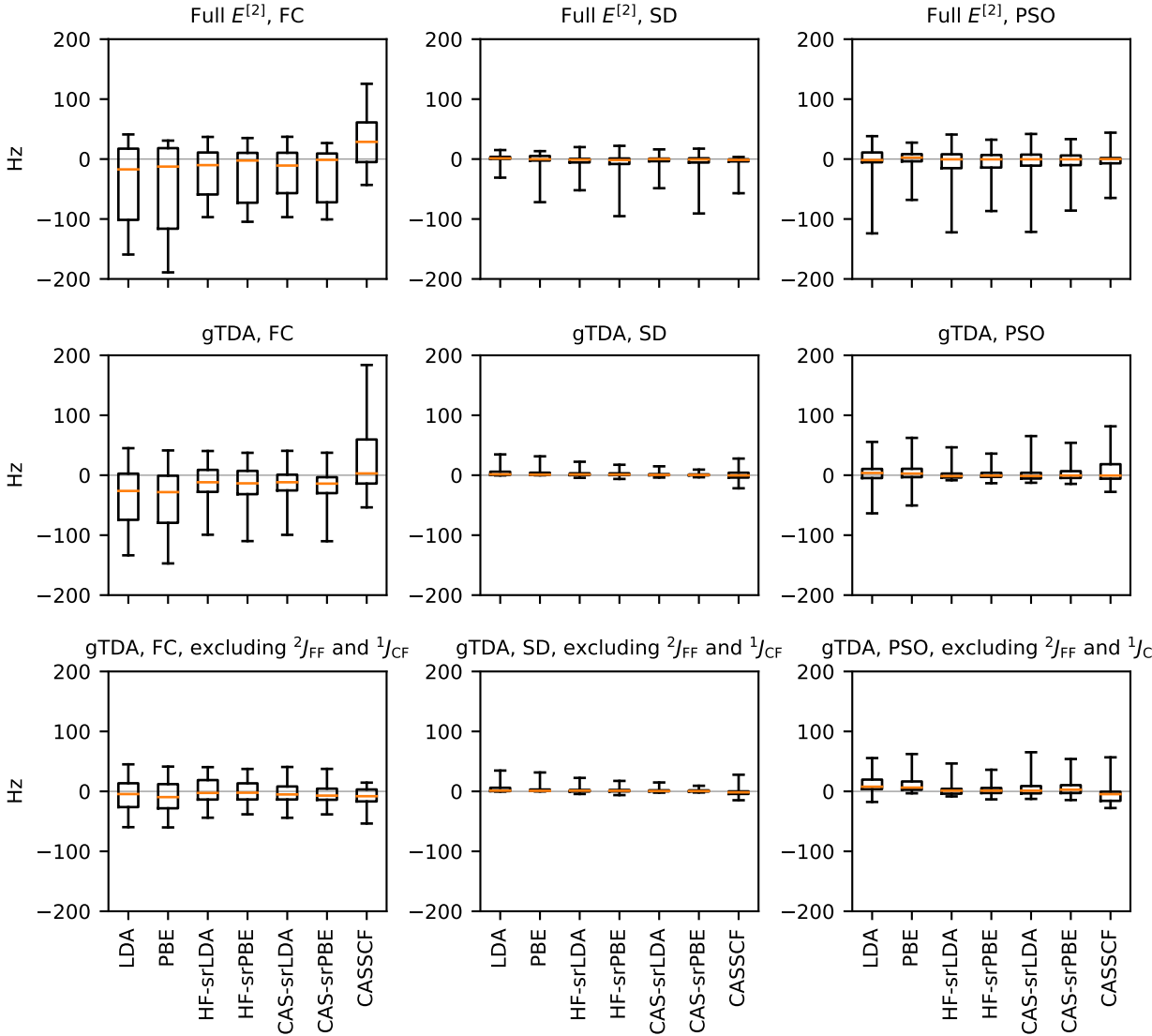
Full $E^{[2]}$, FC
Full $E^{[2]}$, SD
Full $E^{[2]}$, PSO
gTDA, FC
gTDA, SD
gTDA, PSO
gTDA, FC, excluding $^2J_{FF}$ and $^1J_{CF}$
gTDA, SD, excluding $^2J_{FF}$ and $^1J_{CF}$
gTDA, PSO, excluding $^2J_{FF}$ and $^1J_{C}$
Hz
200
100
0
−100
−200
LDA
PBE
HF-srLDA
HF-srPBE
CAS-srLDA
CAS-srPBE
CASSCF

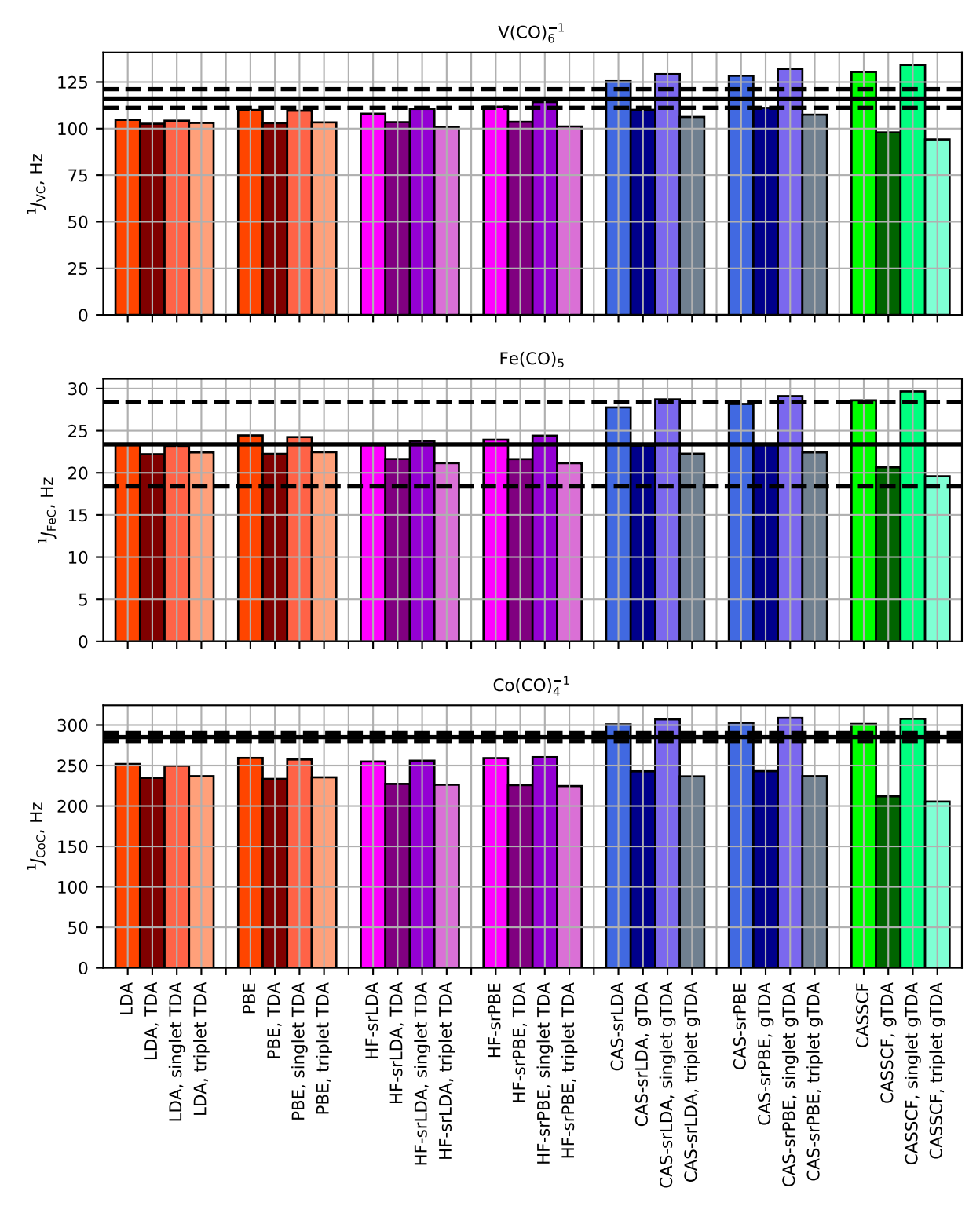
V(CO)$_6^{-1}$
$^1J_{VC}$, Hz
0
25
50
75
100
125
Fe(CO)$_5$
$^1J_{FeC}$, Hz
0
5
10
15
20
25
30
Co(CO)$_4^{-1}$
$^1J_{CoC}$, Hz
0
50
100
150
200
250
300
LDA
LDA, TDA
LDA, singlet TDA
LDA, triplet TDA
PBE
PBE, TDA
PBE, singlet TDA
PBE, triplet TDA
HF-srLDA
HF-srLDA, TDA
HF-srLDA, singlet TDA
HF-srLDA, triplet TDA
HF-srPBE
HF-srPBE, TDA
HF-srPBE, singlet TDA
HF-srPBE, triplet TDA
CAS-srLDA
CAS-srLDA, gTDA
CAS-srLDA, singlet gTDA
CAS-srLDA, triplet gTDA
CAS-srPBE
CAS-srPBE, gTDA
CAS-srPBE, singlet gTDA
CAS-srPBE, triplet gTDA
CASSCF
CASSCF, gTDA
CASSCF, singlet gTDA
CASSCF, triplet gTDA

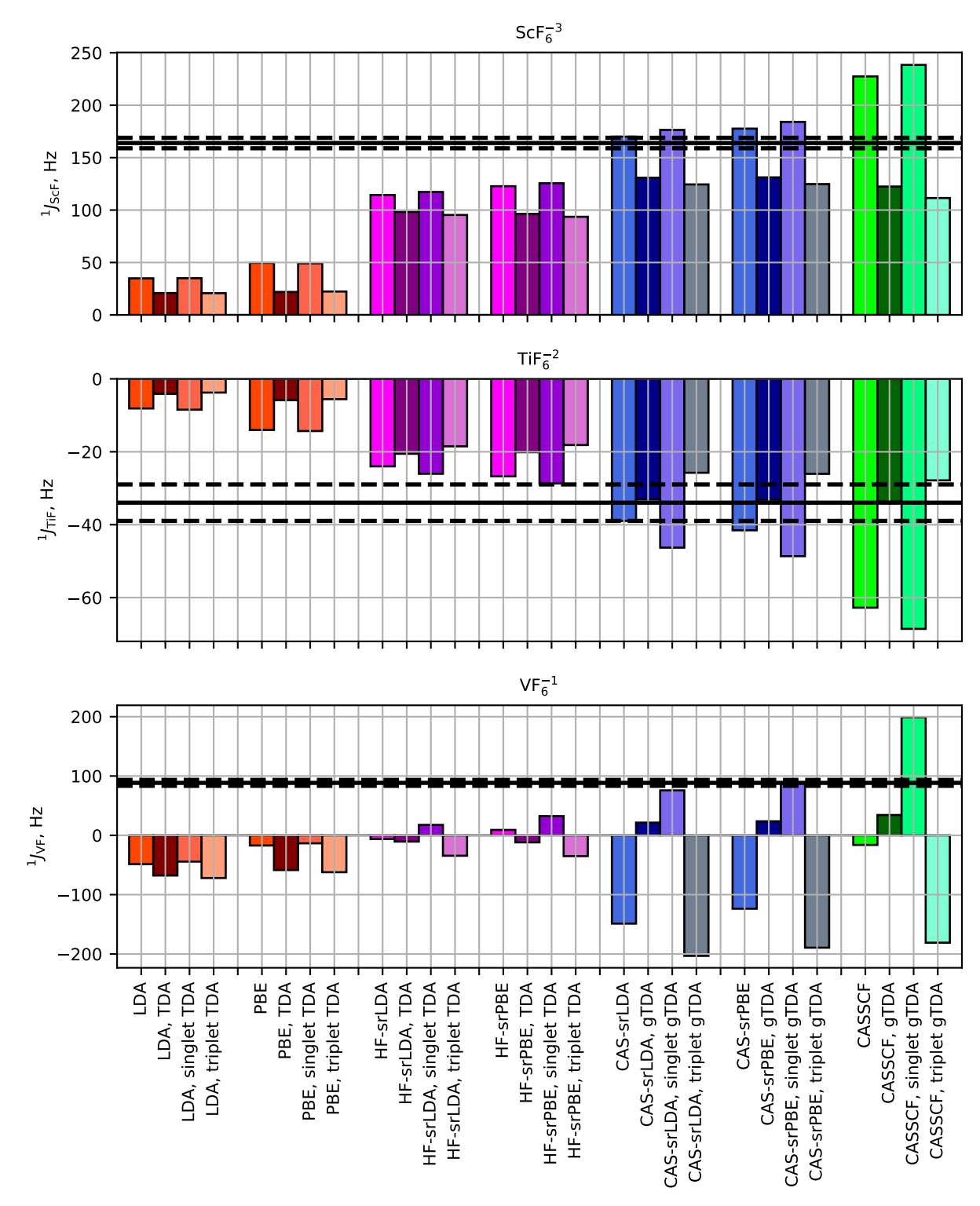
ScF$_6^{-3}$
$^1J_{ScF}$, Hz
250
200
150
100
50
0
TiF$_6^{-2}$
$^1J_{TiF}$, Hz
0
−20
−40
−60
VF$_6^{-1}$
$^1J_{VF}$, Hz
200
100
0
−100
−200
LDA
LDA, TDA
LDA, singlet TDA
LDA, triplet TDA
PBE
PBE, TDA
PBE, singlet TDA
PBE, triplet TDA
HF-srLDA
HF-srLDA, TDA
HF-srLDA, singlet TDA
HF-srLDA, triplet TDA
HF-srPBE
HF-srPBE, TDA
HF-srPBE, singlet TDA
HF-srPBE, triplet TDA
CAS-srLDA
CAS-srLDA, gTDA
CAS-srLDA, singlet gTDA
CAS-srLDA, triplet gTDA
CAS-srPBE
CAS-srPBE, gTDA
CAS-srPBE, singlet gTDA
CAS-srPBE, triplet gTDA
CASSCF
CASSCF, gTDA
CASSCF, singlet gTDA
CASSCF, triplet gTDA